Eclética Química Journal

Original article
iq.unesp.br/ecletica

| Vol. 43 | n. 1 | 2018 |

Study of the thermal behavior in solid state of Mn(II)-Diclofenac Complex

Marcelo Kobelnik[1+], Valdecir Ângelo Quarcioni[2], Adélia Emília de Almeida[3], Clóvis Augusto Ribeiro[4], Marisa Spirandeli Crespi[4+]

[1] Centro Universitário do Norte Paulista (UNORP), São José do Rio Preto, São Paulo, Brazil
[2] Instituto de Pesquisas Tecnológicas (IPT), São Paulo, São Paulo, Brazil
[3] São Paulo State University (UNESP), School of Pharmaceutical Science, Araraquara, São Paulo, Brazil
[4] São Paulo State University (UNESP), Institute of Chemistry, 55 Prof. Francisco Degni St, Araraquara, São Paulo, Brazil

[+] Corresponding authors: Marcelo Kobelnik, e-mail address: mkobelnik@gmail.com
Marisa Spirandeli Crespi, e-mail address: crespims@gmail.com

ARTICLE INFO

Article history:
Received: September 13, 2017
Accepted: April 9, 2018
Published: May 29, 2018

Keywords:
1. Mn(II)-diclofenac complex
2. thermal analysis
3. monotropic reaction
4. activation energy

ABSTRACT: The preparation, characterization and thermal behavior of Mn(II)-diclofenac solid-state complex was investigated by simultaneous TG/DTA and DTG curves, DSC, X-ray powder diffraction (XRD) and scanning electron microscopy (SEM) techniques. The thermal evaluation was carried out with sample masses of 2 and 5 mg, with the purpose of comparing the values of activation energy regarding dehydration, monotropic phase transition and thermal decomposition in both samples mass. The DSC curves were obtained in opened and with crimped lids crucibles of aluminum under oxygen purge gas and static air (without purge gas). The DTA and DSC curves show an exothermic peak between 150-180 °C depending on heating rate, which can be attributed to the monotropic non-reversible reaction. The activation energy (E_a/kJ mol^{-1}) to dehydration, the monotropic phase transition and the first thermal decomposition step were determined by Capela-Ribeiro nonlinear isoconversional method. The activation energy under oxygen dynamic purge gas shows lower values compared to those obtained under static air.

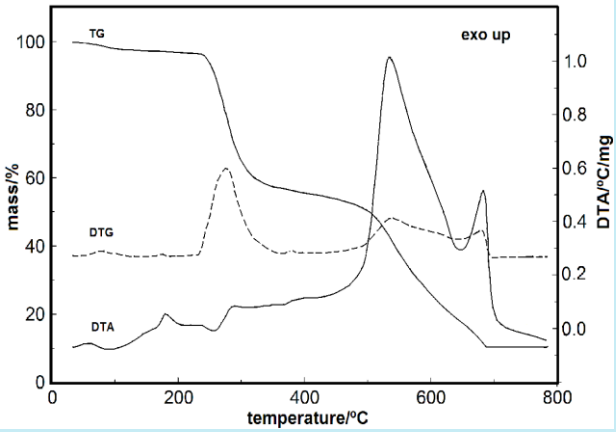

1. Introduction

The diclofenac (2-[2,6-dichlorophenylamino]phenylacetate) is a pharmaceutical drug that can be used as a chemical ligand and has the coordinating ability for complexing several metal ions due to its carboxyl group. The studies of the stable metal complex can be used for different purposes, such as the obtaining metallic oxides to advanced materials (ceramics, glasses, among others) or to obtain new properties of application in biological functions[1-4]. Thus, the thermogravimetry is a valuable technique for studying the thermal behavior of solid-state compounds of metal complexes, which are essential to synthesize complexes in the desired stoichiometry in several applications.

Recently, Kobelnik *et al*. reported the preparation and thermal characterization of a white powder of diclofenac-Sr and Ba compounds, which were evaluated by thermal analysis with two sample masses (2 and 5 mg). The activation energy of dehydration has the similar behavior, but the first and second thermal decomposition stages showed several values of activation energy[5]. Besides, compounds of aluminum and indium (III)[6]

Eclética Química Journal, vol. 43, n. 1, 2018, 59-66
ISSN: 1678-4618
DOI: 10.26850/1678-4618eqj.v43.1.59-66

and cobalt (II)[7] ions were also evaluated by thermal analysis with the aim of obtaining the activation energy by thermal decomposition and phase transition, respectively. In these previous studies[5-7], the activation energy was evaluated with several masses of sample and purge gases to comparison among them.

Thus, as an extension of that works[5-7], the aim of the current work is the study of the thermal behavior and obtaining the kinetics parameters to dehydration, phase transition, and thermal decomposition of Mn (II)-diclofenac complex ($Mn(Diclof)_2$) in the solid-state. The investigations of the dehydration, the first thermal decomposition and a monotropic phase transition (exothermic reaction) of this complex were evaluated by thermogravimetry (TG), differential thermal analysis (DTA) and differential scanning calorimetry (DSC). In addition, to compare the thermal behavior obtained by TG and DSC curves, the analyses were carried out with two different sample sizes and under oxygen purge gas and static condition (without purge gas)[4, 5]. Nevertheless, the monotropic reaction stage (before and after this reaction) was also evaluated by X-ray powder diffraction (XRD) and scanning electron microscopy (SEM). Moreover, the calorimetric evaluation of the complex by DSC curves was carried out under two main conditions: samples in opened and crimped aluminum crucibles to obtain a comparison between the values of activation energy.

1.1 Kinetic Parameters – Nonlinear isoconversional method

The kinetic parameters to the thermal decomposition step of the complex were estimated by Capela-Ribeiro[8] nonlinear isoconversional method, using 4th order rotational approximation of the temperature integral[9]. For a given conversion α and a set of n experiments carried out at different heating rates β_i ($i = 1\ldots. n$), the parameters activation energy, E, and the B term can be determined from Equation 1 minimizing the sum of squares to the plot of heating rate β to each α as function of the $z_i=10^3/RT_i$. ($i = 1\ldots. n$) :

$$S(E.B) = \sum_{i=1}^{n}\left(\beta_i - \frac{\exp(B - Ez_i)}{z_i}\frac{E^3z_i^3 + 14E^2z_i^2 + 46Ez_i + 24}{E^4z_i^4 + 16E^3z_i^3 + 72E^2z_i^2 + 96Ez_i + 24}\right)^2 \quad (1)$$

$$B = ln\left(\frac{10^3A}{Rg(\alpha)}\right) \quad (2)$$

where A is the pre-exponential factor, R is the gas constant, and $g(\alpha)$ represent the reaction mechanism.

2. Experimental

The experimental conditions to the preparation of $Mn(Diclof)_2$ complex is like that previously described[5-7]. A stoichiometric mixing of Mn(II) chloride and potassium diclofenac aqueous soluitons was preapred with continuous stirring until total precipitation of the complex. The precipitate was filtered and washed with water up to the elimination of chloride ion. Then, the solid was dried at room temperature, macerated and stored in a desiccator over anhydrous calcium chloride up to constant mass.

The thermal analysis was performed by simultaneous TG-DTG and DTA using a TA Instruments 2960 SDT, in the 30-400 °C temperature range in open alumina reference and sample pans under a dynamic nitrogen purge gas (flow rate: 100 mL min^{-1}), heating rates of 5, 10 and 20 °C min^{-1} and sample masses of 2 and 5 mg. The stoichiometry evaluation of the complex was obtained by TG curve, using a sample of 7.516 mg in an α-Al_2O_3 crucible, with a heating rate of 20 ºC min^{-1} in synthetic air purge gas with a flow of 100 mL min^{-1}. The kinetic evaluation was carried out by Capela and Ribeiro method[8], and the curves were obtained using heating rates of 5, 10 and 20 ºC min^{-1} and sample masses of around 2 and 5 mg, following the ICTAC Kinetics Committee recommendation[10]. The phase transition was evaluated by DSC curves in a equipament from TA Instruments, DSC 2910 model, between 40 and 200 °C, with heating rates of 5, 10 and 20 °C min^{-1}, aluminum crucible, either open or with crimped lids, in oxygen purge gas (50 mL min^{-1}) or static air.

Eclética Química Journal, vol. 43, n. 1, 2018, 59-66
ISSN: 1678-4618
DOI: 10.26850/1678-4618eqj.v43.1.59-66

The X-ray diffraction patterns (XRD) were performed in a Siemens D-500 X-ray diffractometer using CuK_α radiation (λ = 1.54056 Å) and settings of 40 kV and 30 mA.

The morphology study of this complex was performed by SEM, using a JEOL Scanning Electron Microscope, model JSM-T-330A at an accelerating voltage of 20 kV. The sample was covered with a thin and uniform layer of gold, by sputtering, using a vacuum evaporator.

3. Results and discussion

3.1 Thermal behavior

Simultaneous TG/DTG-DTA curves of hydrated Mn(Diclof)$_2$ are shown in Figure 1. The TG curve of the complex shows that the first mass loss of 2.65 % between 30 and 118 ºC, which can be attributed to the loss of one water molecule, corresponds to the broad endothermic event in DTA curve. The peak is seen in DTA curve between 155 and 182 ºC, having a maximum at 172 ºC, without corresponding mass loss in TG curve. Thus, the material was heated to a temperature immediately higher than the exothermic peak, rapidly cooled and then heated again to verify if this reaction is reversible or not, or if an oxidation reaction occurs. Based on the above information, the exothermic event was attributed to the monotropic phase transition. After heating up to 182 ºC, this monotropic transition was evaluated by XRD (see below Figure 2C), where it is possible to observe the absence of diffraction lines, which can be attributed to a non-crystalline complex.

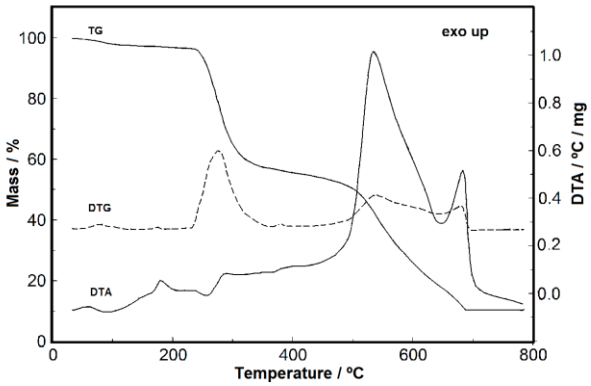

Figure 1. Simultaneous TG/DTG and DTA curves of Mn(Diclof)$_2$.H_2O in synthetic air, sample mass of 7.516 mg, heating rate of 20 ºC min^{-1} in α-Al_2O_3 crucible.

Besides, Figure 1 shows that the complex has loss mass in three steps between 233 and 693 ºC. The first step has a mass loss of 40.02 %, and it is remarkable the presence of a weak endothermic event at 258 ºC. The presence of only one small endothermic event was attributed to the simultaneous reactions, which occur due to the thermal equilibrium between the exothermic and endothermic processes. The second and third steps of thermal decomposition occur between 355 and 693 ºC, and the mass loss is 47.23 %. For this process, two exothermic peaks were observed in DTA curve. The analysis of the final residue, after a total mass loss, is in agreement with the formation of Mn_3O_4, which was confirmed by XRD (residue of Mn_3O_4 from TG: 89.56 % (obtained); 89.67 % (calculated)).

The XRD powder patterns of the complex are shown in Figure 2 (A-C). These analyses reveal that this complex may exist in three conditions: hydrated (Fig. 2A), dehydrated (Fig 2B) and after the monotropic reaction (Fig. 2C). On the other hand, when this analysis was made under nitrogen purge gas after the temperature interval of 182 ºC, (Figure 2 D) it was seen that under this condition the complex is also non-crystalline. SEM micrographs (Figure 3 A-C) show no significant difference in the morphology of the hydrated and dehydrated complex, and after the monotropic phase transition.

Eclética Química Journal, vol. 43, n. 1, 2018, 59-66
ISSN: 1678-4618
DOI: 10.26850/1678-4618eqj.v43.1.59-66

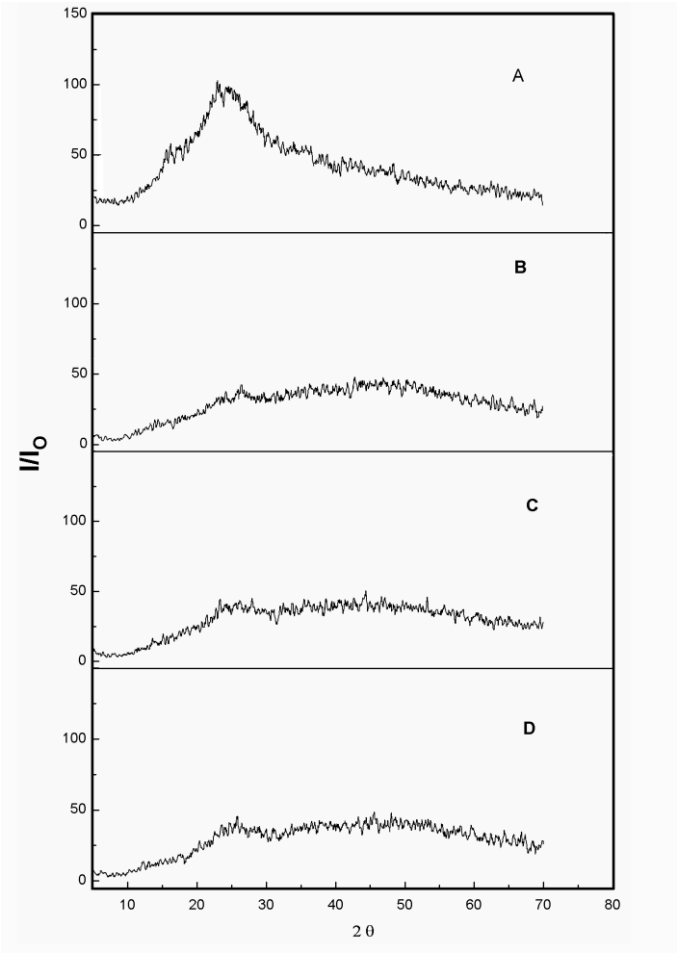

Figure 2. Characteristic parts of X-ray diffraction patterns before (A) and after (B) dehydration step and (C) after the monotropic phase transition. The Fig. 3D corresponding to analysis in nitrogen purge gas, after the monotropic phase transition.

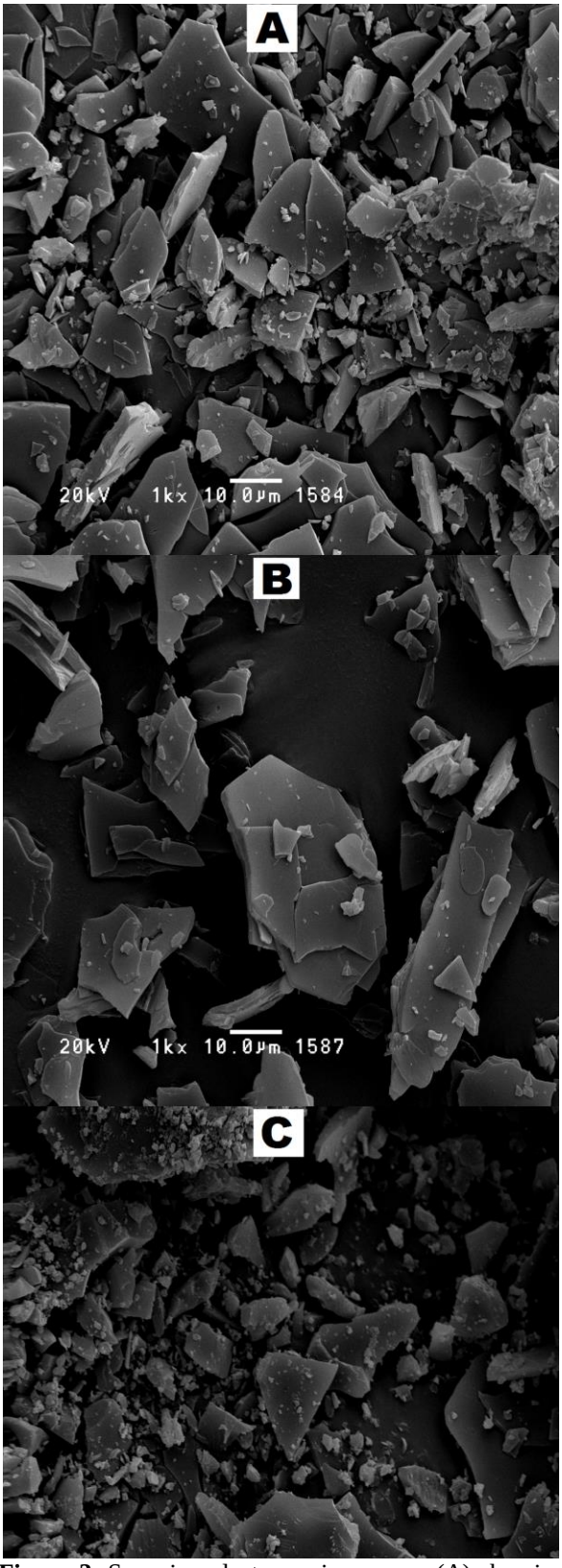

Figure 3. Scanning electron microscopy: (A) showing the $Mn(Diclof)_2.H_2O$ complex; (B) showing the $Mn(Diclof)_2$ complex after dehydration stage and (C) showing the $Mn(Diclof)_2$ complex after the monotropic phase transition.

Eclética Química Journal, vol. 43, n. 1, 2018, 59-66
ISSN: 1678-4618
DOI: 10.26850/1678-4618eqj.v43.1.59-66

Figure 4 shows the TG/DTG curves for 2 mg of $Mn(Dicl)_2.H_2O$ recorded in a nitrogen purge gas, which is an example of the set curves obtained to extract the kinetic parameters. The analyses with 5 mg of the complex were not included due to the significant similarity with the curves in Figure 1 (mass losses are the same: 2 mg = 78.01 % and 5 mg = 78.30 %). These curves show that the mass loss occurs in two steps, being: 1 – the first mass loss attributed to the dehydration in a single stage in the range from 30 to 110 ºC and 2 – the thermal decomposition in the range between 190 and 290 ºC.

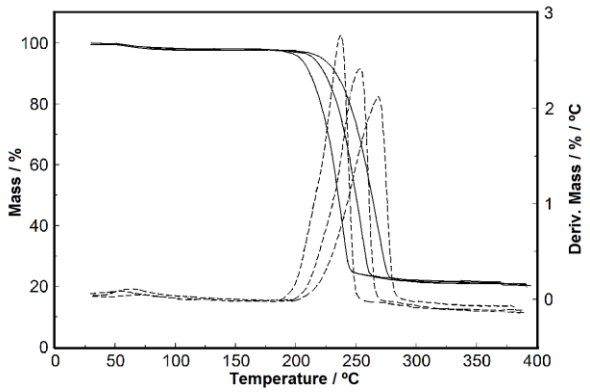

Figure 4. TG/DTG curves of $Mn(Diclof)_2.H_2O$, sample mass around 2 mg, under nitrogen purge gas in α-Al_2O_3 crucible.

The DSC curves (Figures 5 and 6) show the monotropic phase transition in a static air and oxygen purge gas. Both open and crimped lids aluminum crucibles conditions show the same exothermic event between 140 and 180 ºC, which is in agreement with DTA curve, as observed in Figure 1. Another aspect seen on these curves is the difference of displacement in monotropic phase transition peaks under an oxygen purge gas (Figure 5) when the mass of the sample was 5 mg. The peaks shift and became broader. However, under static condition (Figure 6), the peaks are very close to each other, for both masses of the sample, suggesting overlapping reactions. This fact shows that the alteration in the monotropic phase transition in this complex is due to the oxygen conductivity that is favored, while in static air, the reaction does not occur with the same velocity, leading to a broad peak.

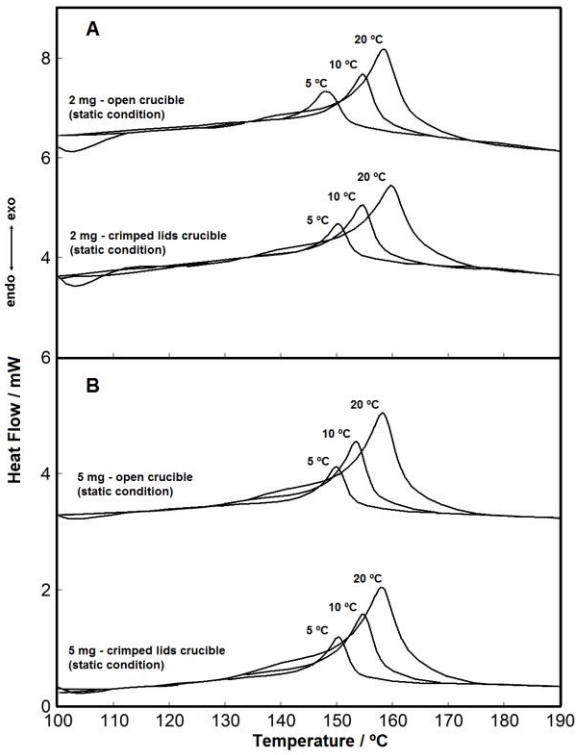

Figure 5. DSC curves in oxygen purge gas, sample mass around 2 mg (A) and 5 mg (B) in open and crimped lids aluminum crucibles.

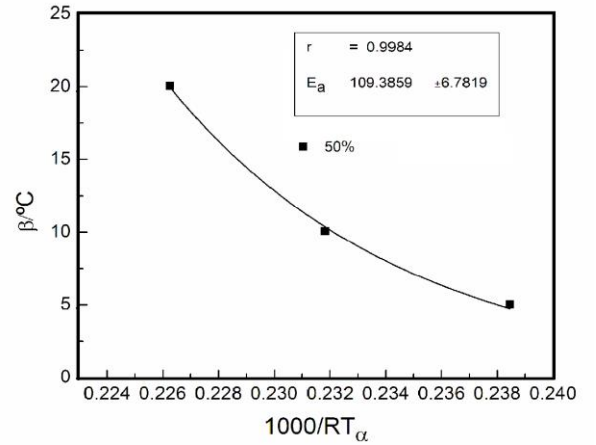

Figure 6. DSC curves in static condition (without purge gas), sample mass around 2 mg (A) and 5 mg (B) in open and crimped lids aluminum crucibles

3.2 Kinetic behavior

The kinetic evaluation of dehydration and thermal decomposition was carried out from three TG curves, with two masses and only in nitrogen purge gas. The kinetic evaluation was also performed by three DSC curves under oxygen purge gas and static condition (without purge gas)[5-7].

Eclética Química Journal, vol. 43, n. 1, 2018, 59-66
ISSN: 1678-4618
DOI: 10.26850/1678-4618eqj.v43.1.59-66

Figure 7 shows the plot of the heating rate (β) as a function of the $1000/RT_\alpha$, obtained from decomposition stage with mass of 2 mg (TG curves), which allows determining the adjustment of activation energy (E_a) for each fixed value of α.

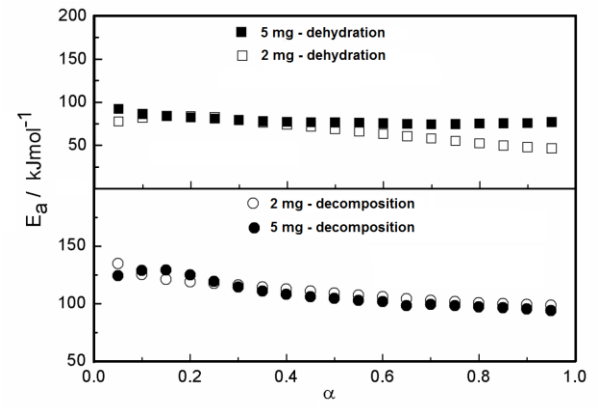

Figure 7. Diagram of β *versus* conversion degree (α - 50 %) in the decomposition step of 2 mg with the adjustment functions.

3.2.1 Dehydration and decomposition stages

The association between the activation energy (E_a) *versus* conversion degree (α) values from dehydration and decomposition stages are shown in Figure 8, and the values of activation energy are shown in Table 1.

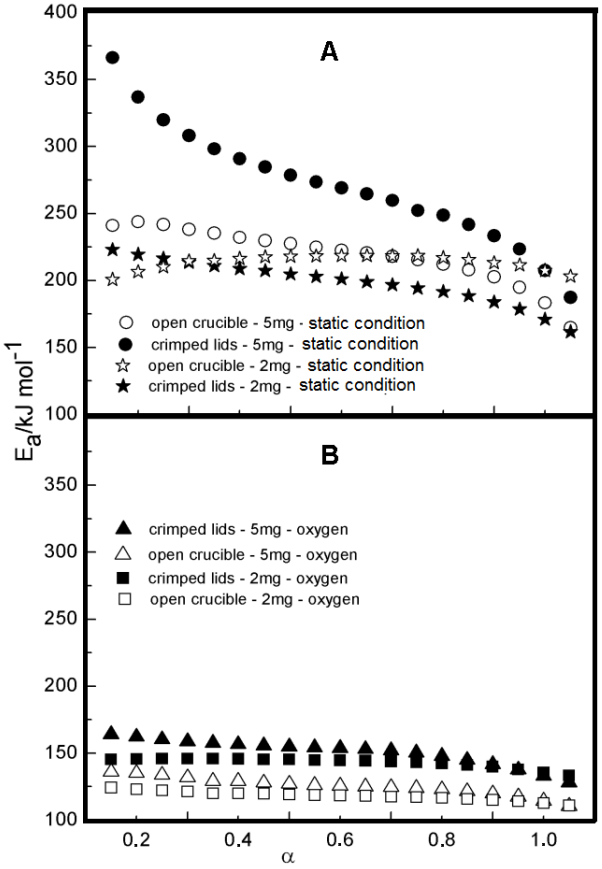

Figure 8. The calculated E_a/kJ mol^{-1} as a function of α for the dehydration and decomposition processes.

Table 1. E_a (kJ mol^{-1}) and correlation coefficient (r) for the dehydration, thermal decomposition and monotropic phase transition

sample mass	*E_a	*r	***sample mass***	*E_a	*r
2 mg dehydration	67.2 ± 0.2	0.99127	2 mg Monotropic reaction (crimped lids) static condition	198.56 ± 0.08	0.99691
5 mg dehydration	77.29 ± 0.06	0.99525	5 mg Monotropic reaction (crimped lids) static condition	270.8 ± 0.2	0.99835
2 mg decomposition	110.7 ± 0.09	0.99810	2 mg Monotropic reaction (crimped lids) oxygen purge gas	142.91 ± 0.03	0.99995
5 mg decomposition	107.8 ± 0.1	0.99716	5 mg Monotropic reaction (crimped lids) oxygen purge gas	150.91 ± 0.06	0.99813

Eclética Química Journal, vol. 43, n. 1, 2018, 59-66
ISSN: 1678-4618
DOI: 10.26850/1678-4618eqj.v43.1.59-66

2 mg Monotropic reaction (open) static condition	213.56 ± 0.02	0.99150	2 mg Monotropic reaction (open) oxygen purge gas	118.21 ± 0.03	0.99964
5 mg Monotropic reaction (open) static condition	218.74 ± 0.09	0.99250	5 mg Monotropic reaction (open) oxygen purge gas	125.37 ± 0.05	0.99982

*Average

For the dehydration step, the samples showed a tendency to maintain the same behavior. In fact, as the water loss is relatively small, the adjustment of the temperatures of the TG curves gives very close results, and therefore, the activation energy values are similar. It occurs when the displacement of the TG or DTG curves is not observed with varying the temperature.

For the thermal decomposition process, the activation energy has a similar behavior for both masses used, but in this case, there was the displacement of the TG curves, which shows that the amount of mass used makes no difference in the kinetic behavior. Also, as observed in DTG curves (Figure 4), the thermal decomposition, for each heating rate, occurs in only one step, that is, without apparent overlapping reactions.

3.2.2 Monotropic phase transition step

The average activation energy values for the monotropic phase transition under static and oxygen purge gases are shown in Table 1. Figure 9 depicts the activation energy *versus* conversion degree (α).

As mentioned above about the behavior of DSC curves, the activation energy values under oxygen purge (Figure 9B) are smaller than in static condition (Figure 9A), but, show the same tendency in both conditions. This demonstrates that the kinetic reaction has the same behavior. In fact, the conductivity of the oxygen associate to the heat flow favors the reaction when compared to static air. This can be proved by the highest activation energy for this last condition using sample mass of 2 mg or 5mg, open or crimped lids aluminum crucible.

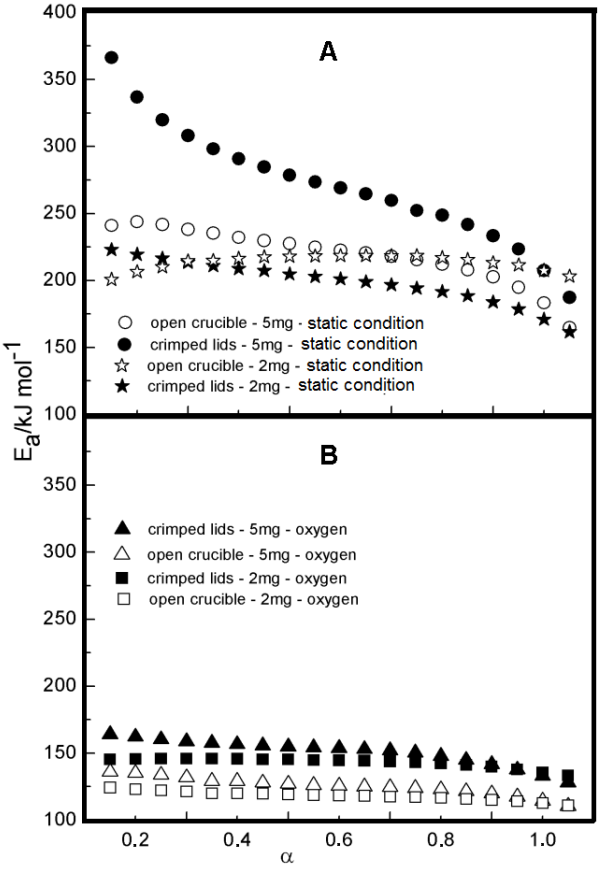

Figure 9, The calculated E_a/kJ mol^{-1} under static condition (without purge gas) (A) and oxygen purge gas (B) as a function of α for the monotropic phase transition

4. Conclusions

The thermal behavior of Mn(II)-diclofenac complex was studied with two sample masses as well as it was established the stoichiometry of this complex as $Mn(Diclof)_2.H_2O$. The thermal evaluation shows steps regarding dehydration, monotropic phase transition, and decomposition which could be evaluated from activation energy values. The results of activation energy for dehydration and decomposition steps showed that

Eclética Química Journal, vol. 43, n. 1, 2018, 59-66
ISSN: 1678-4618
DOI: 10.26850/1678-4618eqj.v43.1.59-66

both samples have similar behavior for the different sample masses used in the assays. The kinetic evaluation of monotropic phase transition showed that activation energy is dependent on the experimental conditions. The XRD patterns show the non-crystalline form and SEM micrograph indicate no significant change in the structure before thermal decomposition.

5. Acknowledgments

CAPES, IPT – Instituto de Pesquisas Tecnológicas do Estado de São Paulo by TG curves and we would like to thank the LME-IQ for the SEM facilities.

6. References

[1] Issa, R. M., Gaber, M., Al-Wakiel, N. A., Fathalla, S. K., Synthesis, Spectral, Thermal and Biological Studies of Mn(II), Co(II), Ni(II) and Cu(II) Complexes with 1-(((5-Mercapto-1H-1,2,4-triazol-3-yl)imino)-methyl)naphthalene-2-ol, Chin. J. Chem. 30 (2012) 547-557. https://doi.org/10.1002/cjoc.201280004.

[2] El-Ghamry, H. A., Sakai, K., Masaoka S, El-Baradie, K.Y., Issa, R. M., Preparation, Characterization, Biological Activity and 3D Molecular Modeling of Mn(II), Co(II), Ni(II), Cu(II), Pd(II) and Ru(III) Complexes of Some Sulfadrug Schiff Bases, Chin. J. Chem. 30 (2012) 881-890. https://doi.org/10.1002/cjoc.201280024.

[3] Khalaji, A. D., Rad, S. M., Grivani, G., Rezaei, M., Gotoh, K., Ishida, H., Cobalt(III) Complex [CoL3] Derived from an Asymmetric Bidentate Schiff Base Ligand L (L=(5-Bromo-2-hydroxybenzyl-2-furylmethyl)-imine): Synthesis, Characterization and Crystal Structure, Chin. J. Chem. 29 (2011) 1613-1622. https://doi.org/10.1002/cjoc.201190241.

[4] Cong, C. J., Hong, J. H., Luo, S. T., Tao, H. B., Zhang, K. L., Kinetics of Thermal Decomposition of Zn1–xMnxC2O4·2H2O in Air, Chin.J. Chem. 24 (2006) 499-503. https://doi.org/10.1002/cjoc.200690096.

[5] Kobelnik, M., Cassimiro, D. L., Dias, D. S., Ribeiro, C. A., Crespi, M. S.,Thermal Behavior of Sr(II) and Ba(II)-Diclofenac Complexes in Solid State: Study of the Dehydration and Thermal Decomposition, J. Chin. Chem. 29 (2011) 2271-2277. https://doi.org/10.1002/cjoc.201180391.

[6] Kobelnik, M., Cassimiro, D. L., Almeida, A. E., Ribeiro, C. A., Crespi, M. S., Study of the thermal behavior of Al(III) and In(III)-diclofenac complexes in solid state, J. Therm. Anal. Cal. 105 (2011) 415-419. https://doi.org/10.1007/s10973-010-1266-y.

[7] Kobelnik, M., Ribeiro, C. A., Dias, D. S., Almeida, S., Crespi, M. S., Capela, J. M. V., Study of the thermal behavior of the transition phase of Co(II)–diclofenac compound by non-isothermal method, J. Therm. Anal. Cal. 105 (2011) 467-471. https://doi.org/10.1007/s10973-010-1208-8.

[8] Cassimiro, D. L., Ribeiro, C. A., Capela, J. M. V., Crespi, M. S., Capela, M. V., Kinetic parameters for thermal decomposition of supramolecular polymers derived from flunixin-meglumine adducts, J. Therm.Anal. Calorim. 105 (2011) 405–410. https://doi.org/10.1007/s10973-010-1116-y.

[9] Capela, J. M. V., Capela, M. V., Ribeiro, C. A., Rational approximations of the Arrhenius integral using Jacobi fractions and gaussian quadrature, J. Mathem. Chem. 45 (2009) 769–775. https://doi.org/10.1007/s10910-008-9381-8.

[10] Vyazovkin. S., Chrissafis, K., Di Lorenzo, M. L., Koga, N., Pijolat, M., Roduitf, B., Sbirrazzuoli, N., Suñol, J. J., ICTAC Kinetics Committee recommendations for collecting experimental thermal analysis data for kinetic computations, Therm. Acta. 590 (2014) 1-23. https:/doi.org/10.1016/j.tca.2014.05.036.

ISSN: 1678-4618
DOI: 10.26850/1678-4618eqj.v43.1.59-66